

# Journal Pre-proof

Engineering more sustainable catalysts based in ecological and economic synthesis routes from renewable raw material: Novel mesoporous silicas for remediation technologies

Eliana G. Vaschetto, Pablo A. Ochoa Rodríguez, Joaquín Pérez Pariente, Griselda A. Eimer

PII: S1387-1811(23)00295-0

DOI: <https://doi.org/10.1016/j.micromeso.2023.112719>

Reference: MICMAT 112719

To appear in: *Microporous and Mesoporous Materials*

Received Date: 16 February 2023

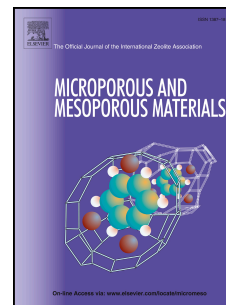
Revised Date: 16 June 2023

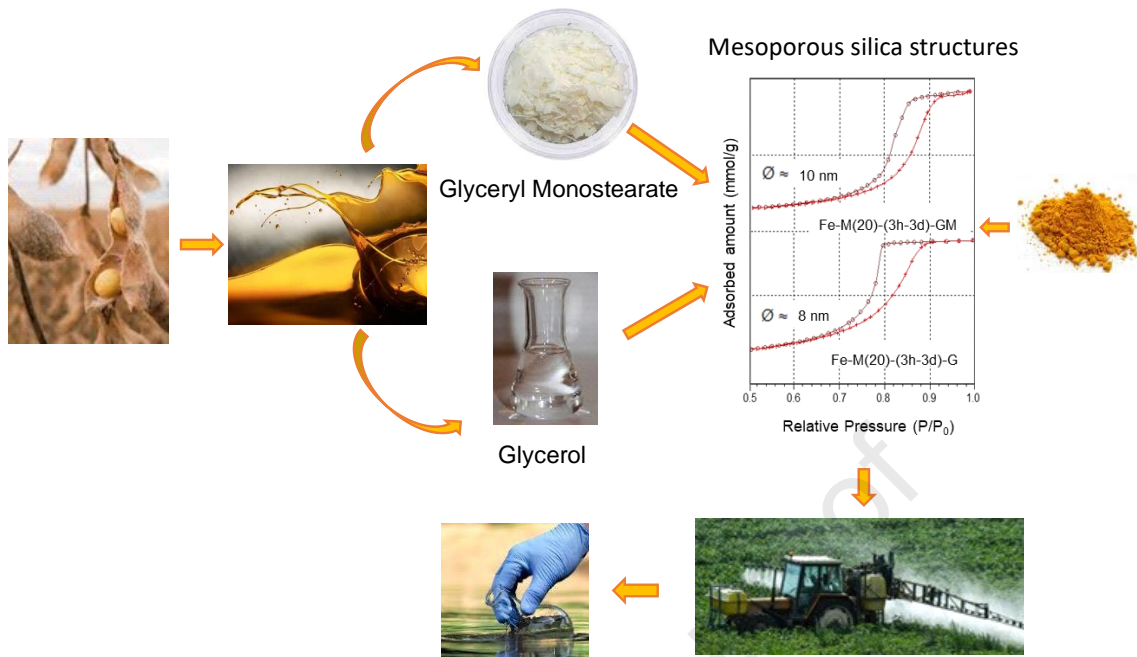
Accepted Date: 1 July 2023

Please cite this article as: E.G. Vaschetto, P.A. Ochoa Rodríguez, Joaquín Pérez Pariente, G.A. Eimer, Engineering more sustainable catalysts based in ecological and economic synthesis routes from renewable raw material: Novel mesoporous silicas for remediation technologies, *Microporous and Mesoporous Materials* (2023), doi: <https://doi.org/10.1016/j.micromeso.2023.112719>.

This is a PDF file of an article that has undergone enhancements after acceptance, such as the addition of a cover page and metadata, and formatting for readability, but it is not yet the definitive version of record. This version will undergo additional copyediting, typesetting and review before it is published in its final form, but we are providing this version to give early visibility of the article. Please note that, during the production process, errors may be discovered which could affect the content, and all legal disclaimers that apply to the journal pertain.

© 2023 Published by Elsevier Inc.





Journal Pre-proof

1        *Engineering more sustainable catalysts based in ecological and economic*  
2        *synthesis routes from renewable raw material: Novel mesoporous silicas for*  
3        *remediation technologies.*

4  
5        Eliana G. Vaschetto<sup>1\*</sup>, Pablo A. Ochoa Rodríguez<sup>1</sup>, Joaquín Pérez Pariente<sup>2</sup>,  
6        Griselda A. Eimer<sup>1\*</sup>.

7  
8        <sup>1</sup> *Centro de Investigación y Tecnología Química (CITeQ-UTN-CONICET), Facultad*  
9        *Regional Córdoba, Maestro López y Cruz Roja Argentina, Ciudad Universitaria,*  
10        *5016 Córdoba, Argentina. Tel: +54-351-4690585.*

11        <sup>2</sup> *Instituto de Catálisis y Petroleoquímica, ICP-CSIC, C/ Marie Curie 2, 28049,*  
12        *Madrid, España.*

13  
14        \*[geimer@frc.utn.edu.ar](mailto:geimer@frc.utn.edu.ar)  
15        \*[elivaschetto@hotmail.com](mailto:elivaschetto@hotmail.com)  
16

17        Abstract

18        Iron modified mesoporous silica structures were achieved from biomass-derived  
19        renewable molding agents (glyceryl monostearate and glycerol) and can become  
20        potential substitutes for conventional mesoporous catalysts synthesized from  
21        petrochemical-derived precursors. These materials were prepared by different  
22        methods (wet impregnation with iron contents of 2.5, 5, 10 and 20% w/w and direct  
23        incorporation using a molar ratio Si/Fe=20) and characterized by XRD, N<sub>2</sub>  
24        adsorption and desorption isotherms, UVvis-DR and ICP. By using these solid as  
25        heterogeneous catalysts in the wet oxidation reaction of the herbicide glyphosate  
26        with air under extremely mild reaction conditions (atmospheric pressure and room  
27        temperature), herbicide degradation / fragmentation levels of around 70% were  
28        achieved. The methodology employed for the synthesis played a key role in the  
29        development of the structure and dispersion of Fe species as well as in the stability  
30        of the catalytic system. In this way, an advanced technology with low  
31        environmental impact for the treatment of a pollutant of great concern at the global

1 level was developed, which adds sustainability to the chemical industry from the  
2 use of residual glycerol and/or glyceryl monostearate in the catalyst synthesis.

3  
4 *Keywords:* Renewable porogens, mesoporous silicas, glyphosate degradation.

## 5 6 1. Introduction

7 In 1992, siliceous ordered mesoporous materials of the MCM-41 type began to be  
8 synthesized [1], using commercial molding agents/surfactants/templates. Their  
9 characteristics, such as large specific surface (in the order of 1000 m<sup>2</sup>/g), highly  
10 porous and ordered structure (pore diameters between 2 and 10 nm) and high pore  
11 volume (up to 1.3 cm<sup>3</sup>/g), are the main properties responsible for these materials  
12 having a high adsorption capacity even for bulky molecules [2]. By modifying  
13 mesoporous materials with different metals [2,3], catalysts suitable for many  
14 chemical reactions have been developed. On the other hand, the final structure of  
15 the material depends on a series of factors, such as metal concentration,  
16 hydrothermal treatment, synthesis time, among others. Since the preparation of  
17 these siliceous catalysts was reported, there has been intense research activity on  
18 their synthesis. Various ionic and neutral surfactants that act as template or  
19 structure-forming agents have been evaluated as a simple but innovative technique  
20 for the production of nanomaterials of different classes [2-5]. However, these  
21 surfactants are expensive and environmentally unfriendly due to low  
22 biodegradability, further requiring frequently the use of toxic solvents as swelling  
23 agents or long time of heating to expand the pore size. These characteristics  
24 make industrial-scale applications of mesoporous silica disadvantageous.  
25 Therefore, there is a need of alternate synthesis approach which should be  
26 inexpensive, robust, easily handled and efficient [6]. Hence, the development of  
27 more ecological and economical synthetic routes, such as the use of surfactants or  
28 porogens from renewable resources, remains a challenge in the field of the  
29 synthesis of these solids. Currently, there is renewed interest in the synthesis of  
30 mesoporous silica-based materials driven by a new approach that puts emphasis  
31 on the use of biologically derived materials found in nature or extracted from

1 biomass resources [7]. Many biomass materials exhibit hierarchical large-scale  
2 order and self-assembly properties that can be replicated in a variety of structures;  
3 hence, the use of biomass materials as alternative to commercial surfactants and  
4 precursors not only yields materials with structural diversities but also holds  
5 promise for the low-cost synthesis of biocompatible materials [7].

6 Canlas and Pinnavaia [8] reported the utilization of naturally derived oleyl amine  
7 surfactants for the synthesis of worm-like and lamellar mesoporous silica. These  
8 structures are similar to those obtained using petroleum-based alkyl amine  
9 surfactant.

10 Thomas et al. [9] reported the use of surfactant formulations based on glutamic  
11 acid and leucine containing a mixture of lauryl amino acid and fatty acid for the  
12 formation of mixtures of ordered mesoporous silica including lamellar phases [10].

13 Likewise, sodium N-dodecyl glycine and potassium N-dodecyl glycine amino  
14 acid-based surfactants prepared by reacting coconut oil amine with  
15 monochloroacetic acid in alkali medium were used to synthesize hexagonal and  
16 cubic structures [11].

17 Also, various polysaccharide-based polymers have been used as templates to  
18 direct the synthesis of silica, including chitosan, chitin colloids and cellulose [12-  
19 14]. However, these efforts yielded poorly ordered materials after template removal  
20 by calcination.

21 Recently, mesoporous KIE-6 (Korea Institute of Energy-6) was synthesized using  
22 crude glycerol and sulfuric acid. However, a pre-calcination step at 150°C for 2 h  
23 was necessary to prevent the escape of the pore-forming glycerol before the  
24 formation of a rigid network by silanol group condensation. Otherwise, glycerol is  
25 evaporated before condensation resulting in reduced pore size and volume in the  
26 calcined composites [15].

27 In order to replace petroleum based surfactants, overcoming the difficulties  
28 encountered so far in this aim, this paper deals with the use of oleochemical  
29 industry derived glycerol (G) and glyceryl monostearate (GM) as porogens cheap  
30 and highly available in Argentine from the production of biodiesel [16]. In addition,  
31 these non-ionic molding agents have advantages, such as: easy removal,

1 tendency to produce structures with thicker walls and smaller particle size solids,  
2 which would improve the porosity and stability of the material. These  
3 characteristics make them extremely interesting for use in the synthesis of  
4 mesoporous silicas with enhanced industrial and technological applications.

5 On the other hand, in recent years there have been great advances in the field of  
6 chemistry, with the synthesis of many new substances, including plastics, drugs,  
7 petroleum products, fertilizers and pesticides. The production and use of these  
8 substances have improved human living conditions leading to population growth;  
9 however, the development of the synthetic chemical industry presents great  
10 contradictions for the environment due to the release of large amounts of organic  
11 and inorganic substances whose effects on the environment are sometimes  
12 unknown. One of the main environmental contaminants are pesticides, which  
13 involve a very extensive group of chemicals, among which herbicides stand out.  
14 These are widely used in agriculture in order to control the growth of weeds or  
15 herbs, being applied to plants or soils, which can cause contamination of aquatic  
16 systems. The most important factors in the transport of herbicides towards natural  
17 water bodies are aerial dispersion by winds, volatilization and dragging by  
18 rainwater and irrigation, which cause damage or adverse effects to aquatic  
19 organisms, constituting a major environmental problem. One of the most widely  
20 used agrochemicals herbicides is glyphosate ( $C_3H_8NO_5P$ ) [17,18]. The great  
21 solubility of herbicides in water means that, when they are applied to the soil, they  
22 can diffuse into surface or groundwater generating severe contamination. The low  
23 mobility of glyphosate in soil would indicate minimal contamination of groundwater;  
24 however, it may reach surface water after direct use in the vicinity of aquatic  
25 environments or seepage after land application [19,20]. In this context, Advanced  
26 Oxidation Processes (AOPs) are proposed as a degradation alternative for this  
27 type of compounds in aqueous media. It has been shown that the addition of a  
28 solid catalyst to the system can promote the formation of radicals on the surface,  
29 speed up the reaction rate and improve the efficiency, drastically reducing the  
30 severity of the operating conditions [19,20]. In this context we already have  
31 demonstrated the efficiency of modified mesoporous catalysts based in SBA-15

1 silica for the degradation/fragmentation reaction of glyphosate in aqueous media  
2 through wet oxidation processes with air [21,22].

3 In this work, promoting the use of biomass as raw material for the catalyst  
4 synthesis, Fe-modified mesoporous silicas prepared by employing G and GM as  
5 porogens have been catalytically evaluated in the degradation of glyphosate in  
6 aqueous media. By this way, it may be envisaged the large-scale development of  
7 mesoporous materials with a reasonable cost and relatively less impact on the  
8 environment [7]. The interesting results achieved in this work allow us to propose a  
9 more sustainable advanced technology for the treatment of water contaminated  
10 with herbicides.

## 11 12 2. Experimental

### 13 2.1 Synthesis of materials.

14 The catalysts were synthesized by two procedures: wet impregnation and direct  
15 incorporation of the metal in the synthesis gel. By using the direct incorporation  
16 method, tetraethoxysilane (TEOS, Aldrich, 98%) was used as Si source, glycerol  
17 (G Cicarelli, 99.5%) or glyceryl monostearate (GM, Sigma Aldrich) as template or  
18 porogen agent, and ethanol as solvent. Hydrochloric acid (2M, Cicarelli, 36.5-38%)  
19 was used as a pH regulator (pH=2), sodium fluoride (Sigma Aldrich, P.A.) to start  
20 the silica condensation reaction and ferric chloride as source of Fe. The pure  
21 mesoporous silica synthesis procedure [23] involves an initial stage where a  
22 solution of the porogen in ethanol with another solution of TEOS and HCl are  
23 mixed under magnetic stirring at 60°C. In a second stage, the condensation of the  
24 silica is carried out by adding the NaF salt at 60°C. For the synthesis of the  
25 materials modified with Fe, at this moment, the necessary amount of Ferric  
26 chloride (Sigma Aldrich,  $\geq 98\%$ ) to reach a nominal molar ratio Si/Fe=20 is  
27 incorporated, keeping the agitation for 1, 3 or 5h at 60°C. The composition of the  
28 gel was: Si : HCl : ethanol : H<sub>2</sub>O : GM = 1 : 4 : 34 : 92 : 0.2 for catalysts  
29 synthesized from glyceryl monostearate, and for those synthesized from glycerol:  
30 Si : HCl : ethanol : H<sub>2</sub>O : GM = 1 : 4 : 34 : 92 : 5. Finally, the gel obtained was  
31 thermally treated at 85 °C in autoclave reactors for 1, 3 or 5 days. The samples

1 were dried at 60 °C and subsequently the template agent was evacuated by  
2 calcination with air flow at a controlled temperature (550 °C for 1h). The solids  
3 synthesized via direct incorporation were identified as Fe-M(20)(xh-yd)-G or Fe-  
4 M(20)(xh-yd)-GM where “x” corresponds to hours of agitation of synthesis gel and  
5 “y” to days of hydrothermal treatment.

6 By the wet impregnation method, 0.25 g of calcined pure siliceous support  
7 synthesized using GM or G were impregnated, using a rotary evaporator at 60°C  
8 and 80 rpm, with solutions of Ferric chloride in 2.5 g of ethanol in order to reach  
9 nominal metal contents of 2.5, 5, 10 or 20 % w/w. The solids were dried at 60 °C  
10 overnight and finally calcined at 350 °C for 3h. These materials were identified as:  
11 Fe/M(z)-GM or Fe/M(z)-G where "z" symbolizes the nominal Fe content in % w/w.  
12 Siliceous matrices were identified as M-GM or M-G.

13

14 2.2 Characterization of materials.

15 An X'Pert Pro PANalytical Polycrystal RX Diffractometer was used, collecting data  
16 between  $2\theta = 0.5-6$  (small-angle) and  $10-90^\circ$  (wide-angle).

17 Surface area, pore size distribution, and pore volume were determined from N<sub>2</sub>  
18 adsorption-desorption isotherms using ASAP 2420 Micromeritics equipment after  
19 degassing the samples at 130 °C for 16 h under vacuum. The surface area was  
20 determined by the Brunauer-Emmett-Teller (BET) method. Pore size distribution  
21 and average pore diameter were determined by the Barrett-Joyner-Halenda (BJH)  
22 method applied in the adsorption branch of the isotherm.

23 The scanning electron microscopy (SEM) images of the materials were obtained in  
24 a FeSEM Karl Zeiss - Sigma. Gold coverage was applied to make samples  
25 conductive. Moreover, the solids were analyzed by Transmission Electron  
26 Microscopy (TEM) with a JEOL JEM-2100 Plus, working voltage: 200 kV. A small  
27 drop of the dispersion (sample in solution water-ethanol 50%) was deposited on  
28 copper grid and then evaporated in air at room temperature.

29 The Fe content in the synthesized materials was determined using the Inductively  
30 Coupled Plasma Optical Emission Spectroscopy (ICP-OES) technique in a  
31 PlasmaQuant PQ 9000 Analytik Jena equipment.



1 To determine iron speciation as a function of metal content, UVvis diffuse  
2 reflectance (UVvis DR) spectra were recorded using a Jasco 650 spectrometer  
3 with an integrating sphere in the 200-900 nm wavelength range. The original  
4 spectra obtained were fitted by several Gaussian bands using the conventional  
5 least squares method.

6

### 7 2.3 Catalytic evaluation

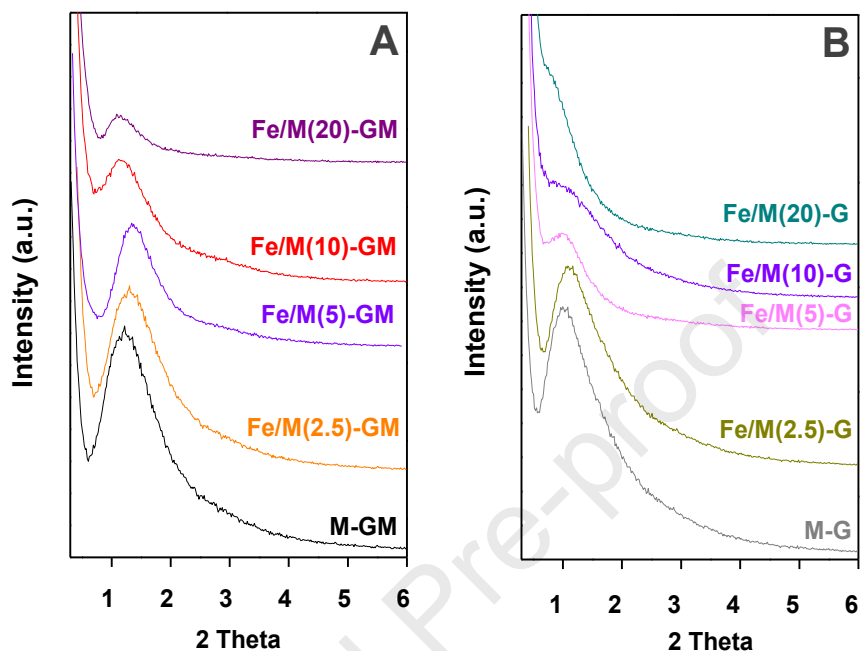
8 The solids were catalytically evaluated in the glyphosate degradation reaction by  
9 wet oxidation with air. An 8 mm diameter and 35 cm long glass fixed bed down-  
10 flow 2-neck reactor was used, operating at room temperature and atmospheric  
11 pressure and using 0.2 g of the catalyst. A solution of glyphosate in water (15 ppm)  
12 was fed to the reactor by syringe pump (10 ml/h), and air used as oxidant was  
13 introduced through the upper side path (30 ml/min). The samples were analyzed by  
14 ion chromatography (Dionex ICS-1100, 5890 Series II Plus, Ion Pac AS18 Anionic  
15 Column, AG18 Column Guard and KOH as eluent). Degradation products (acetate,  
16 nitrate, nitrite and phosphate) were identified by comparison with chromatographic  
17 standards [21,22]. The degradation percentage was calculated as  $X = (C_0 - C) \times$   
18  $100/C_0$ , where C: concentration of glyphosate and  $C_0$ : initial concentration. The  
19 reaction samples were taken every 15 min.

20

### 21 1. Results and Discussion

22 The small-angle X-ray diffraction patterns of the silica supports and catalysts  
23 synthesized by the wet impregnation method (Figure 1 A-B) showed in all cases a  
24 characteristic pattern of mesoporous materials (signal at 2 Theta around 1-2°) [2,  
25 21,22]. It can be observed that these patterns are less defined according to the  
26 increase in Fe loadings, accentuating this characteristic for the materials  
27 synthesized with G and higher Fe loadings (Figure 1B). Furthermore, corrosive  
28 treatment with  $FeCl_3$  during impregnation and further calcination could likely lead to  
29 structural rearrangement. This fact would be consistent with the observed slipping  
30 for the main XRD peak towards small angles and could contribute to less-defined  
31 XRD patterns as Fe loadings increase. Despite the last statements, it should be

1 remarked that both renewable porogens derived from biomass allow achieving a  
2 mesoporous structure.



16 **Figure 1.** Small-angle XRD patterns of silica support and materials synthesized by  
17 the wet impregnation method using: **A)** GM and **B)** G.

19 Figure 2 shows the wide-angle X-ray diffraction patterns of the materials, where a  
20 broad peak at 2 Theta between 20-30° assigned to amorphous silica is detected  
21 [23]. It is also observed that all Fe loaded samples present peaks corresponding to  
22 the presence of iron oxides which appear more defined and with greater intensity  
23 for the highest Fe loadings. These diffraction peaks are distinctive of hematite,  
24 Figure 2A [24]. Thus, the presence of hematite formed on the external surface of  
25 the synthesized materials could be corroborated. In addition, the silica supports show  
26 two peaks at 2 Theta: 33° and 46° which can be attributed to the presence of sodium  
27 chloride. Such compound can arise from the NaF and HCl used for the synthesis of the  
28 catalysts [25, 26].

29  
30

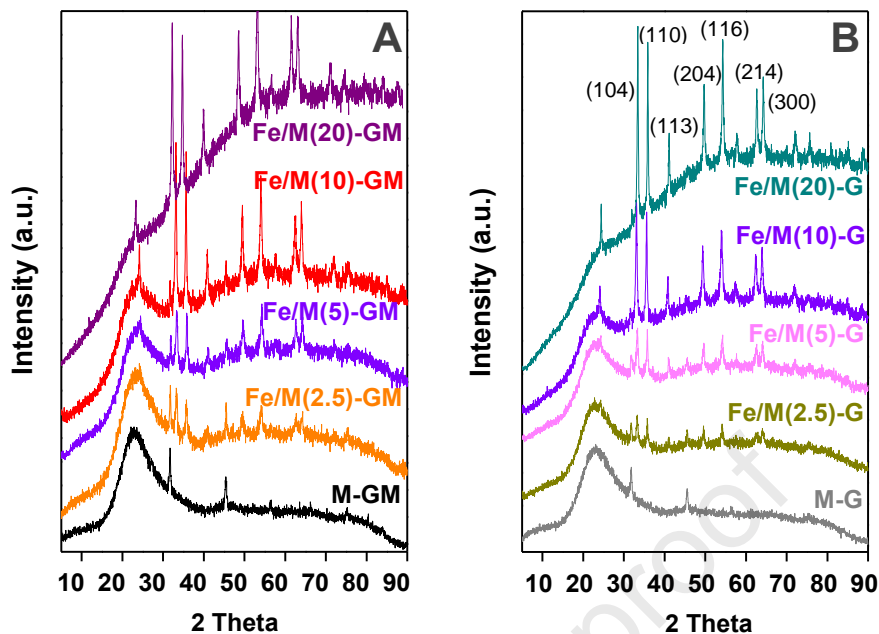
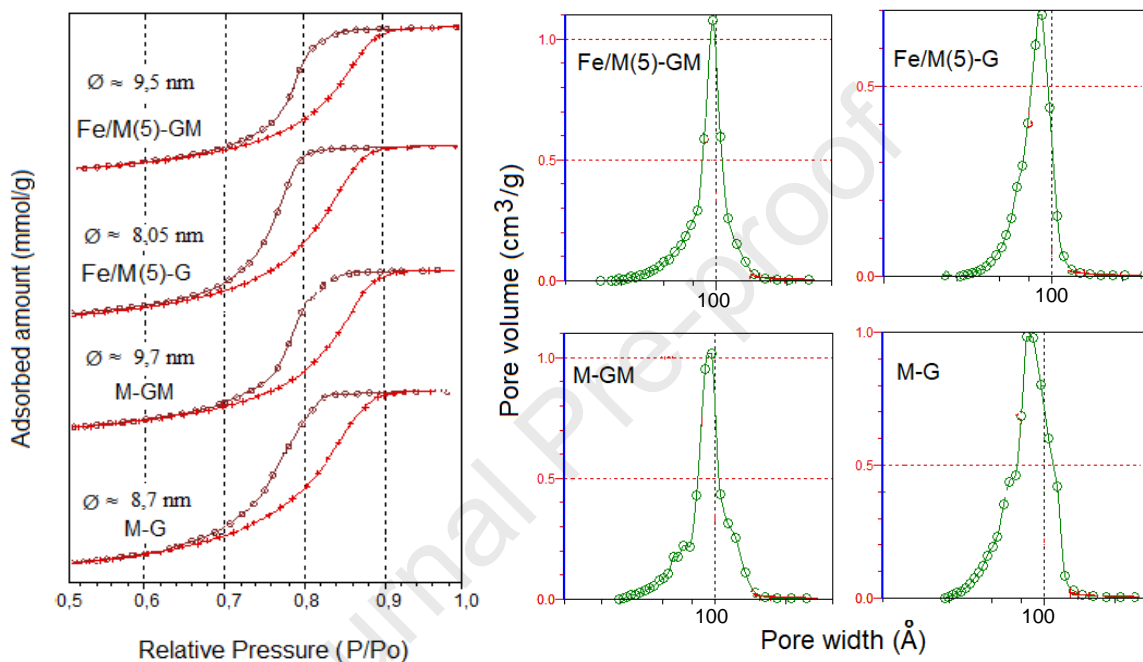


**Figure 2.** Wide-angle XRD patterns of materials synthesized by the wet impregnation method using: **A)** GM and **B)** G. Between parenthesis were identified the diffraction planes corresponding to the  $\text{Fe}_2\text{O}_3$  hematite phase, (330664, Joint Committee on Powder Diffraction Standards).

The  $\text{N}_2$  physisorption was carried out in order to complete the information about the structure of the samples. The adsorption–desorption isotherms and the corresponding pore size distributions of representative samples synthesized using wet impregnation are shown in Figure 3. These can be classified as IV type being typical of mesoporous structures, where the hysteresis curves exhibited a marked inflection for a relative pressure of around 0.7 to 0.85 ( $P/P_0$ ) characteristic of capillary condensation within the mesopores [27]. Pore diameters of the order of 8–9.7 nm typical of mesoporous materials were observed. Accordingly, the mesoporosity of these solids make them potential candidates as materials to replace conventional mesoporous catalysts synthesized from petrochemical industry-derived precursors. It should be noted that the porogens used in this synthesis generate pore diameters larger than those resulting from traditional template agents such as cetyltrimethyl ammonium bromide/chloride (template for MCM-41 that generates pores of the order of 2–4 nm) and Pluronic (non-ionic

1 surfactant used in the synthesis of SBA-15 that produces 5-7 nm pores). Using  
 2 glycerol and glyceryl monostearate (both molecules with similar chemical nature),  
 3 pore diameters in the range of 8 - 8.7 nm and 9.5 - 9.7 nm were achieved,  
 4 respectively. The difference in the pore size between both materials may be related  
 5 to the size of the molecules of the template agents used [16]. These results are  
 6 consistent with the specific area values of around 200-400 m<sup>2</sup>/g (Table 1).



7  
8  
9  
10  
11  
12  
13  
14  
15  
16  
17  
18  
19  
20  
21 **Figure 3.** Isotherms and pore size distribution of representative samples:  
 22 Fe/M(5)-GM, Fe/M(5)-G, M-GM and M-G.

23  
24 Regarding the results of the Fe contents, determined by ICP, they ranged between  
 25 2 and 20 wt. %. depending on the metal amount used in the impregnation (Table 1)  
 26 in consistency with the expected nominal Fe loadings.

27  
28  
29  
30

**Table 1.** Physicochemical properties of the synthesized solids and glyphosate degradation values.

Sample	Area (m <sup>2</sup> /g)	Fe content (wt. %) <sup>a</sup>	Glyphosate degradation(%) <sup>b</sup>
M-GM	347	0	1.5
Fe/M(2.5)-GM	305	2.09	28
Fe/M(5)-GM	338	4.45	44.5
Fe/M(10)-GM	386	10.06	48.46
Fe/M(20)-GM	390	20.9	60
M-G	338	0	0
Fe/M(2.5)-G	205	2.1	38.11
Fe/M(5)-G	226	4.56	54.6
Fe/M(10)-G	267	9.96	64.72
Fe/M(20)-G	289	19.8	66.15

<sup>a</sup> By ICP

<sup>b</sup> By ionic liquid chromatography (time on stream: TOS=15 min)

Measurements of transmission electron microscopy of the materials were made in order to examine their structural regularity. TEM images of representative samples are shown in Figure 4.

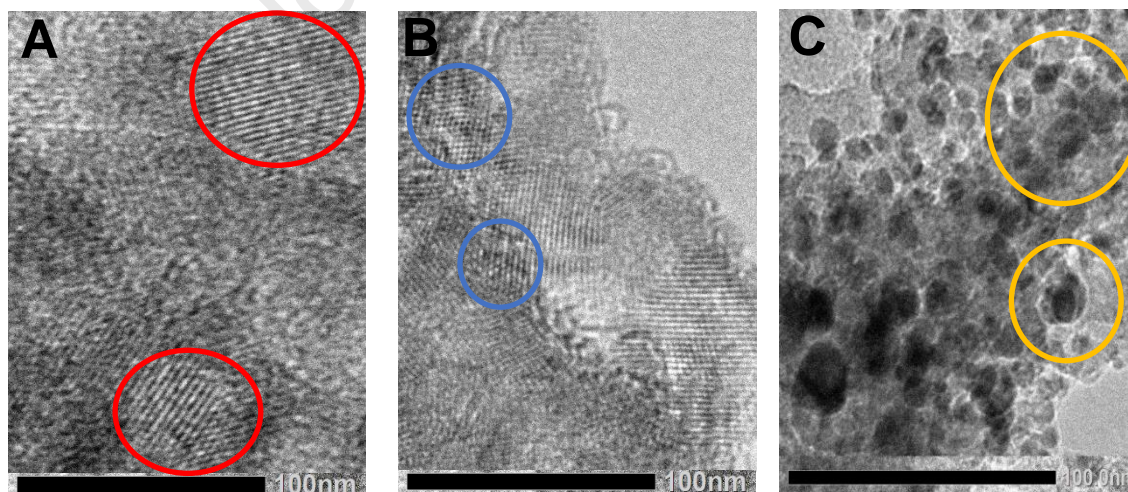


**Figure 4.** Transmission electron microscopy of representative samples prepared by impregnation: A) M-GM, B) Fe/M(2.5)-GM, C) Fe/M(20)-G

1

2 The materials presented a defined mesoporous structure, exhibiting zones whose  
3 ordering is characteristic of a hexagonal pore arrangement [2]. It should be noted  
4 that in Figure 4A the image is viewed perpendicularly to the direction of the pore  
5 arrangement, clearly showing the presence of straight mesochannels arraying  
6 along the long axis [2]; meanwhile, the hexagonal arrangement of the unidirectional  
7 mesopores is clear in Figure 4B where a frontal view of them can be seen. In this  
8 Figure, the presence of Fe oxides within of the mesochannels can be inferred from  
9 the dark spots of the channels size (see figure area indicated by circles). In  
10 addition, Figure 4C would seem to indicate the presence of segregated oxides,  
11 judging by areas of high contrast larger than the mesopore size.

12

13

14

15

16

17

18

19

20

21

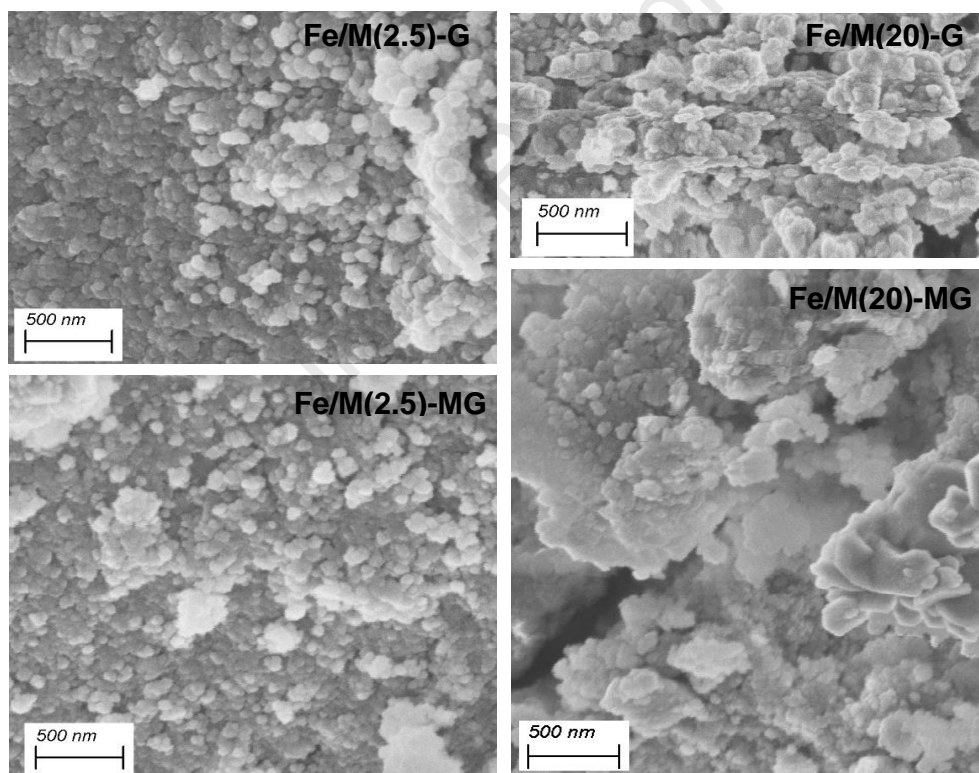
22

23

24

25

26



27 **Figure 5.** Scanning electron micrographs of representative samples prepared by  
28 impregnation.

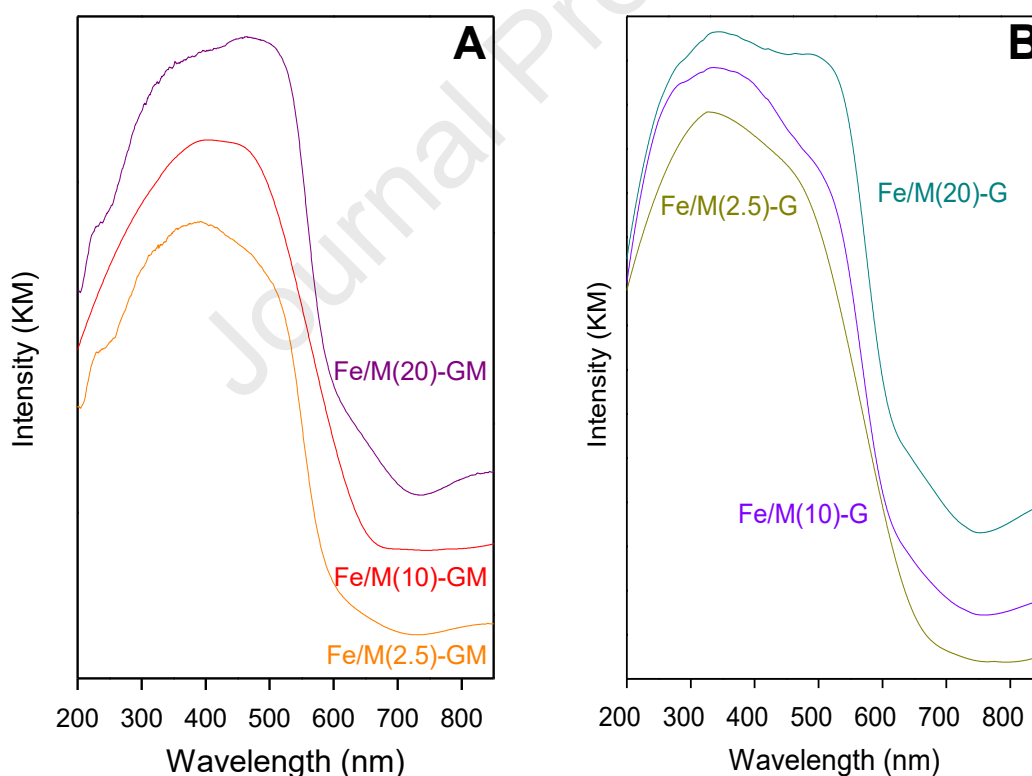
29

30 The SEM images of some samples taken as representative are shown in Figure 5.

31 These images indicate the presence of particles that do not display any particular

1 crystalline habit or morphology, although the spherical-like morphology seems to  
2 be the dominant one. The primary particles are very small and appear to be  
3 aggregated into larger secondary particles which exist in various sizes. Thus, these  
4 particles could be the result of intergrowth of multiple smaller particles [2].

5 The UV-vis DR spectroscopy is a useful method for studying the chemical  
6 environment and electronic state of transition metal ions in silica frameworks [28-  
7 33]. It was applied here to infer about the nature of iron species grown in  
8 mesoporous silicates modified with different Fe loadings. The UV-vis DR spectra of  
9 the samples synthesized with 2.5 and 20 wt.% iron nominal loading and using GM  
10 and G are shown in Figure 6. As it is known, absorption in the 220-300 nm range is  
11 associated to the transitions with ligand to metal charge transfer (CT) character  
12 involving isolated framework iron cations ( $\text{Fe}^{+3}$  ions) while the contributions  
13 detected at longer wavelengths are related with d-d transitions [30,31,34-36].



29 **Figure 6.** UV spectra of representative samples prepared by impregnation.

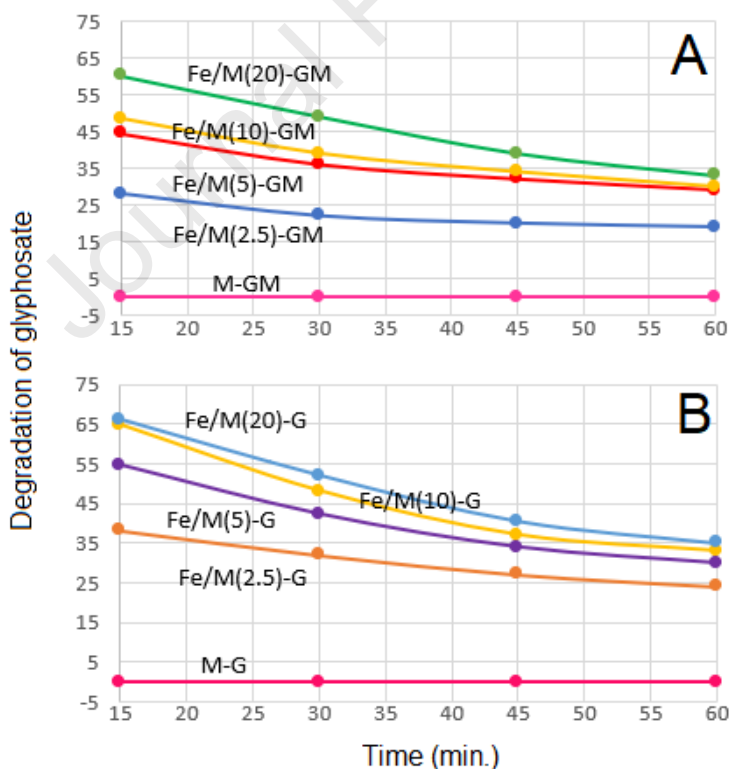
1 According to literature [30,31,34-36], spectra characterized by a broadening and  
2 marked increase in the absorbance of the CT band at longer wavelength,  
3 extending and overshadowing the d-d transitions region, can be related with the  
4 presence of  $\text{Fe}^{+3}$  species with different coordination states (tetrahedral and  
5 octahedral). Thus, some literature data indicate that octahedral  $\text{Fe}^{+3}$  present in  
6 small oligonuclear clusters shows strong and broad absorptions between 300 nm  
7 and 450 nm [30,31,34-35]. Meanwhile a broad absorption at wavelengths greater  
8 than 450-500 nm has been considered to arise from  $\text{Fe}^{+3}$  species present in cluster  
9 of increased size or massive oxidic aggregates such as iron oxide nanoparticles  
10 [34-40]. It is important to note that the absorption capacity of the solids presented  
11 in this work is consistent with the metal content. Thus, the materials with higher  
12 loadings present more intense signals throughout the range of wavelengths  
13 though the shape of spectra is some different. An increase in absorbance is  
14 observed at longer wavelengths with a shift of the absorbing edge for samples with  
15 higher Fe content. This feature is accounting for the increased formation of  $\text{Fe}^{+3}$   
16 species in extraframework positions such as larger size iron oxide cluster and/or  
17 nanoparticles (trapped in the channels or their intersections or segregated outside  
18 the channels). In agreement, the XRD patterns of the most Fe loaded samples  
19 showed more intense peaks corresponding to the presence of iron oxides  
20 (hematite).

21 The materials synthesized by wet impregnation were catalytically evaluated in the  
22 glyphosate degradation reaction (Table 1). The catalysts with the highest Fe  
23 content led to the greatest degradation of the herbicide, of the order of 60% and  
24 66% (after 15 min of reaction) for the solids synthesized using GM and G,  
25 respectively. Under conditions of atmospheric pressure and room temperature, the  
26 fragmentation of the herbicide towards the ions: acetate, nitrate, nitrite and  
27 phosphate (characterized by ionic liquid chromatography) was achieved. The pure  
28 siliceous matrices did not show degradation of the herbicide, evidencing that the  
29 activity of the solids is referred to the presence of Fe. Glyphosate is known to form  
30 stable complexes with metallic cations [41-44]. In these complexes the oxygen of  
31 the phosphonate and carboxylate groups and even the nitrogen atom of the amino



1 group (if it is not protonated) can coordinate to the central metal. [18,21, 45-47]. As  
 2 it was proposed by us elsewhere [21,22] (in accordance with Sheldon and Kochi  
 3 [48,49]) Fe-glyphosate complex formed on the solid can activate molecular oxygen  
 4 and, with the contribution of protons of the reaction medium, generate an active  
 5 oxoiron(V) intermediate. From this, the mechanism of oxygen transfer to the  
 6 substrate (glyphosate adsorbed) could be started, leading to its fragmentation and  
 7 further desorption of the degradation products [21]. In this way, Fe cations in the  
 8 mesoporous silica structure can act efficiently as metal centres responsible of  
 9 glyphosate complex formation and beginning of oxygen transfer to substrate. Their  
 10 increased presence in the synthesized catalysts with highest Fe loadings would be  
 11 justifying the higher activity for Fe/M(20)-GM and Fe/M(20)-G solids.

12 Figure 7 shows the degradation percentages of the herbicide over time on stream  
 13 for the different catalysts synthesized. In all cases, a decrease in the glyphosate  
 14 degradation/fragmentation curve over time is observed.



30 **Figure 7.** Glyphosate degradation as a function of time using solids impregnated  
 31 with Fe and siliceous matrix.

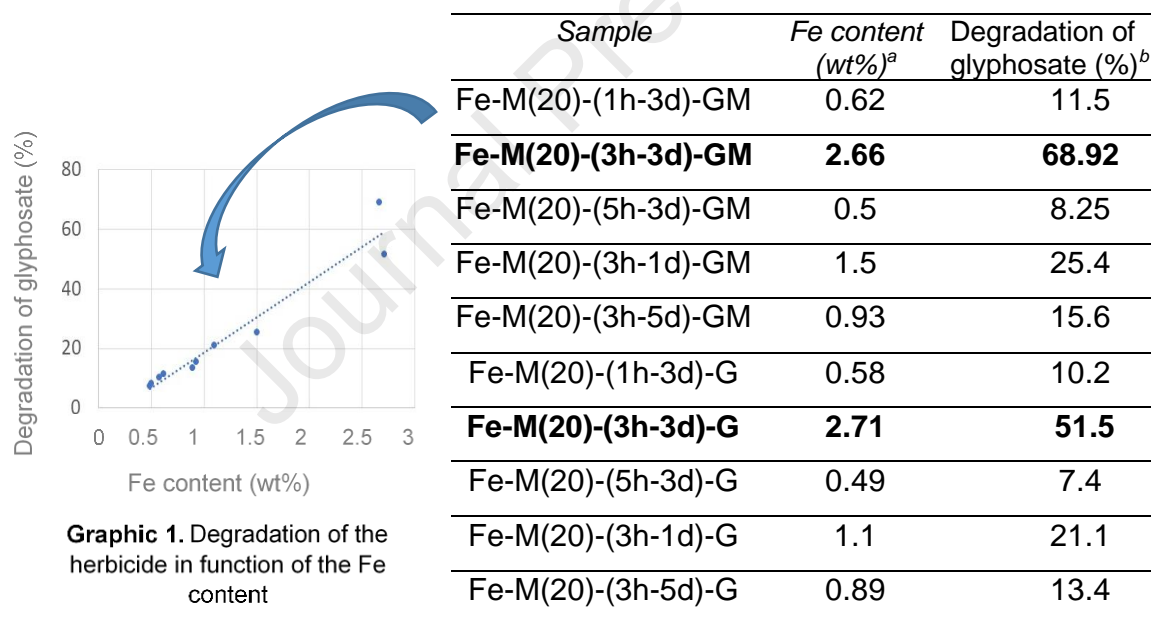
1

2 For the materials synthesized with GM (Figure 7A) the degradation values at 60  
 3 min decrease up to around 20-35%. This feature can be attributed to the leaching  
 4 of Fe from the structure on the time, thus losing catalytic efficiency. For example,  
 5 the content of Fe for the Fe/M(20)-GM after use reached a 8.8 wt. %. This fact is  
 6 also evidenced by the yellowish color of the collected product samples after the  
 7 first 15 min of reaction, confirming the reason why glyphosate fragmentation  
 8 decreased markedly over time. A similar behavior was evidenced for the catalysts  
 9 synthesized from glycerol as molding agent (Figure 7B).

10

11 **Table 3.** Physicochemical properties of the solids synthesized by direct  
 12 incorporation and glyphosate degradation values.

13



14 **Graphic 1.** Degradation of the  
 15 herbicide in function of the Fe  
 16 content

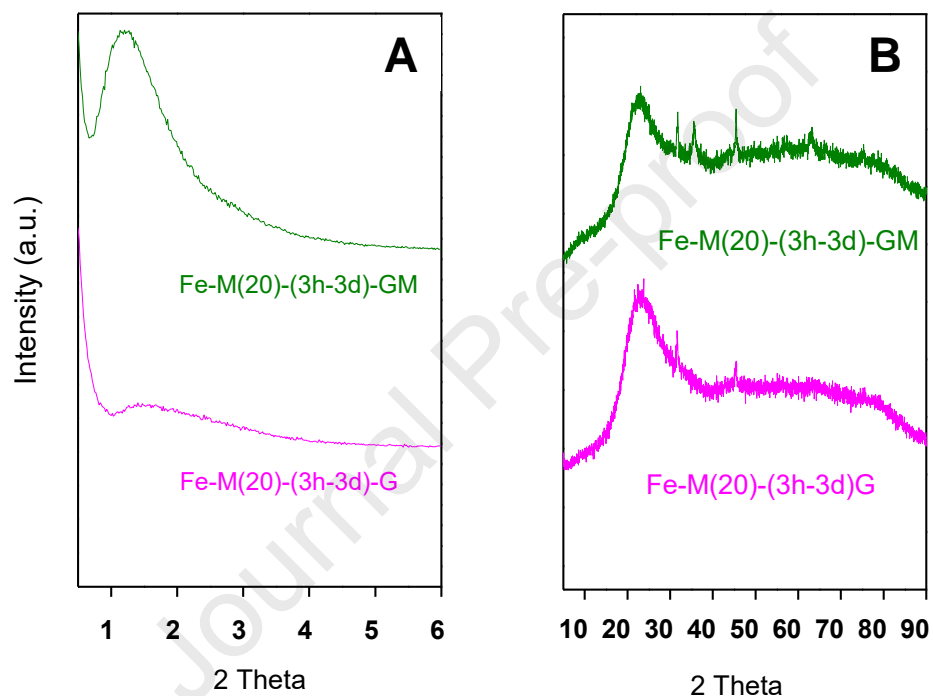
14

15 <sup>a</sup> By ICP16 <sup>b</sup> By ionic liquid chromatography (TOS=15 min)

17

18 As it is known, the synthesis methodology of direct incorporation of metal into the  
 19 initial gel with the adequate adjustment of the synthesis variables can favor, in  
 20 general, a greater anchoring of metal species on the silica than the post-synthesis  
 21 methodology of metal impregnation, causing a marked decrease in leaching. Thus,

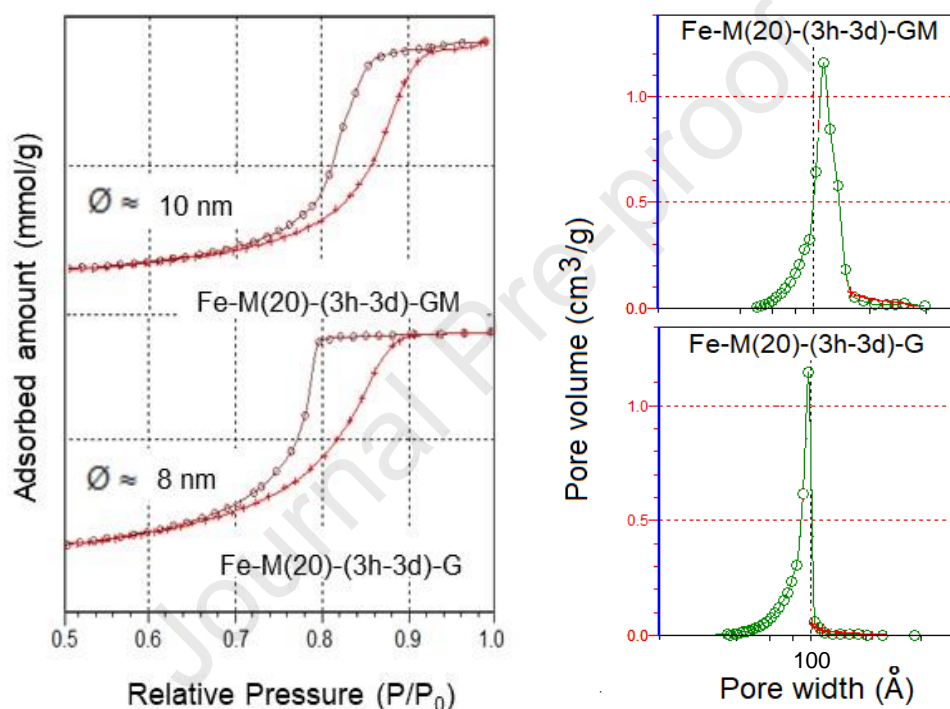
1 the method of direct incorporation of Fe into the solids was also analyzed in this  
2 work. In addition, taking into account that lower Fe loadings incorporated by  
3 impregnation seem to decrease the leaching of Fe from solid, a Fe content of 2.5  
4 wt. % was select to incorporate into the silica matrix by direct synthesis. Thus, by  
5 tailoring synthesis variables as agitation time (h) and hydrothermal treatment time  
6 (days), an optimum nominal molar ratio of Si/Fe= 20 was found to achieve a Fe  
7 content of about 2.5 wt. % in a solid prepared by direct incorporation.



22 **Figure 8: A)** Small-angle XRD patterns and **B)** Wide-angle XRD patterns of: Fe-  
23 M(20)-(3h-3d)GM and Fe-M(20)-(3h-3d)G.

24  
25 Table 3 shows the Fe contents in the solid synthesized by direct incorporation with  
26 molar ratio Si/Fe= 20 of the starting gel, and the corresponding glyphosate  
27 degradation percentages obtained in their catalytic evaluation. The higher  
28 incorporation of Fe (using both porogens) was achieved by 3h of initial gel agitation  
29 and 3 days of hydrothermal treatment at 85°C. Under these conditions (3h of initial  
30 gel agitation and 3 days of hydrothermal treatment), the mesoporous structure was  
31 reached, according to XRD (Figure 8) and N<sub>2</sub> adsorption/desorption isotherms

1 (Figure 9). Nevertheless, it should be noted that using G as surfactant, under the  
 2 same conditions, the structural regularity evidenced by XRD is deteriorated (Figure  
 3 8A). Furthermore, the lack of peaks or barely hinted peaks assignable to an iron oxide  
 4 crystalline phase in the wide-angle XRD pattern (Figure 8B) indicates that the  
 5 developed metal species would be amorphous or have a size under the detection limit of  
 6 the XRD technique. Again, the peaks at 2 Theta:  $33^\circ$  and  $46^\circ$ , attributed to the  
 7 presence of sodium chloride probably arising from NaF used for the synthesis, can be  
 8 observed [25,26].



23 **Figure 9.** Isotherms and pore size distribution of samples: Fe-M(20)-(3h-3d)-GM  
 24 and Fe-M(20)-(3h-3d)-G.

26 Newly, the TEM images (Figure 10) reveal a well-defined mesoporous structure  
 27 with hexagonal arrangement of mesopores, without the presence of oxides  
 28 segregated from the structure. Likewise, dark spots of the channels size (see figure  
 29 area indicated by circles) would be accounting for the presence of finely dispersed  
 30 Fe species within the channels.

31

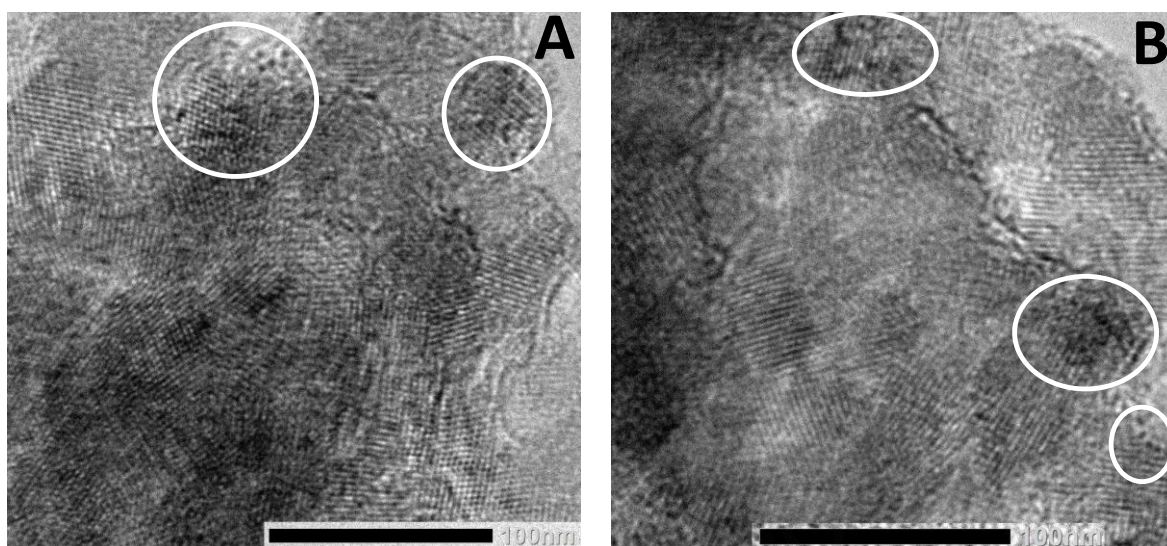
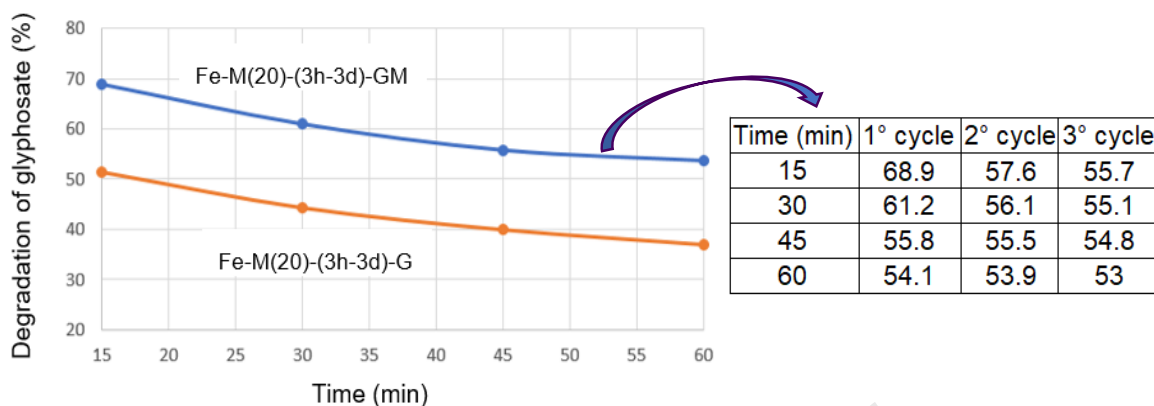


**Figure 10.** Transmission electron microscopy of representative samples prepared by impregnation: A) Fe-M(20)- (3h-3d)-GM, B) Fe-M(20)- (3h-3d)-G

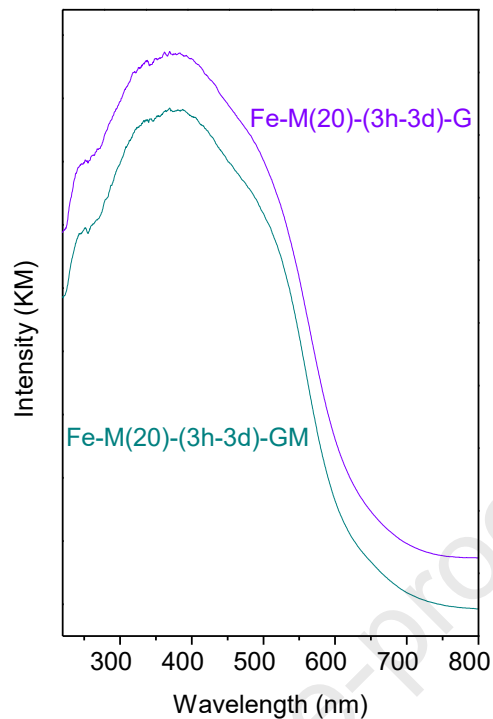
With respect to the catalytic activity results (Figure 11), with these materials it was possible to increase the degradation of glyphosate after 15 min up to around 70% and 50 % by using Fe-M(20)- (3h-3d)-GM and Fe-M(20)-(3h-3d)-G, respectively, in comparison with values of 28 and 38 % obtained by using solids with similar Fe content synthesized by wet impregnation. Moreover, it should be noted that a practically linear relationship is observed between the degradation of the herbicide and the Fe content (graph 1 of Table 3), which would indicate that the activity per iron atom is the same in all the samples, regardless of the variation of synthesis conditions and of the porogens used. This fact would confirm that the same type of active centers was achieved for all the samples. Figure 11 shows the catalytic evaluation results over time on stream using the materials synthesized by direct incorporation. For these solids, the degree of decrease in degradation over time was less than for the solids synthesized by impregnation. In fact, as previously mentioned, the direct incorporation would favor the anchoring of the active metal species in the structure, making them more resistant to leaching.



9 **Figure 11.** Degradation of glyphosate of reaction time (Fe-M(20)-(3h-3d)-GM and  
10 Fe-M(20)-(3h-3d)-G), and degradation in 3 catalytic cycles using Fe-M(20)-(3h-3d)-  
11 GM.

12  
13 On the other hand, the UV spectra of samples synthesized by this methodology  
14 (shown in Figure 12) show an intensity decrease of the absorption above 450 nm  
15 [28,29,40]. This feature suggests that larger size iron oxide clusters and/or  
16 nanoparticles would be contributing less heavily than in the case of the solids  
17 synthesized by impregnation. This feature has already been demonstrated by XRD  
18 and TEM. Probably the minor presence of clustered iron species and consequently  
19 the higher Fe dispersion achieved by direct synthesis would be one of the causes  
20 that is favoring the higher activity of these solids.

21 In addition, the best result obtained with the solid Fe-M(20)-(3h-3d)GM could also  
22 be related to its pore diameter,  $\text{\AA} \approx 10$  nm (Figure 7) caused by using GM as  
23 molding agent. Smaller pore diameters of around 8 nm (Figure 7), evidenced by  
24 adsorption-desorption isotherms of  $\text{N}_2$ , were obtained by using G. The larger pore  
25 diameter of the material would facilitate the formation of voluminous oxo-iron (V)  
26 intermediaries, generated from the glyphosate - Fe complex on the solid capable of  
27 activating the  $\text{O}_2$  of air, which promote the degradation/fragmentation of the  
28 herbicide [21,22].



1  
2 **Figure 12.** UV spectra for the materials synthesized by direct incorporation.

3  
4 An important aspect to be studied in a catalytic process is the stability of the  
5 catalyst over the time on stream as well as the possibility of recycling. In order to  
6 check the recycling ability of catalyst under the reaction conditions, three recycling  
7 experiments were carried out for Fe-M(20)-(3h-3d)GM. After each reaction, the  
8 catalyst was recovered and calcined at 500 °C for to be reused. It should to be  
9 noted that a negligible difference in the catalyst mass was determined after each  
10 cycle, suggesting that the presence of non-volatile species adsorbed on catalyst  
11 surface, which could poison the active sites, is very low [50]. Then, for the three  
12 cycles, the glyphosate degradation shows almost constant values of around 54%  
13 for a time on stream of 60 min. Likewise, for the third cycle, these values also  
14 remain practically constant over time. (Figure 11). In this way, the materials  
15 engineering used for the design of mesoporous catalysts based on renewable  
16 molding agents, would allow to provide sustainability to the synthesis processes of  
17 materials with projection to their commercialization in the chemical industry. Thus,  
18 the direct synthesis methodology proposed in this work gives rise to simpler, more

1 ecological, with lower-cost procedures that are more suitable for industrial  
2 applications of the solids, such as their use in advanced technologies for the  
3 herbicides degradation from polluted water.

4 Finally, although we have already found high values of glyphosate degradation by  
5 using Fe/SBA-15 synthesized via a conventional method [21,22], the degradation  
6 values obtained here are very relevant, considering the importance of the use of  
7 renewable raw materials in the sustainability and economy of the processes.

8

## 9 Conclusion

10 Fe modified mesoporous materials were successfully synthesized from renewable  
11 molding agents, glyceryl monostearate and glycerol, by wet impregnation and  
12 direct incorporation methods. Both biomass-derived porogens allow a mesoporous  
13 structure to be achieved which was corroborated by XRD and physisorption of N<sub>2</sub>.  
14 Thus, these solids are presented as potential substitutes for conventional  
15 mesoporous catalysts synthesized from precursors derived from petrochemical  
16 industry.

17 The materials were catalytically evaluated in the glyphosate degradation through  
18 wet oxidation reaction with air. While catalysts synthesized by Fe impregnation  
19 lead to high levels of degradation but decaying over reaction time, those  
20 synthesized by Fe direct incorporation present higher levels of degradation which  
21 are maintained through reaction time. This methodology leads to Fe species more  
22 finely dispersed, more accessible and strongly anchored in mesoporous structure  
23 providing the catalytic system with greater stability and activity. The best result  
24 (around 70% of glyphosate degradation after 15 min of reaction) was obtained by  
25 using a solid prepared by direct incorporation with molar ratio Si/Fe = 20, GM as  
26 porogen, 3h of initial gel agitation and 3 days of hydrothermal treatment at 85°C.  
27 Finally, material engineering applied to the development of advanced remediation  
28 technologies allowed the degradation of a pollutant of great global concern as  
29 glyphosate towards less toxic and more biodegradable molecules (mainly short-  
30 chain ions) under mild reaction conditions (1 atm and room temperature).

31



## 1 Acknowledgements

2 EGV and GAE are research members of CONICET, Argentina. Authors are  
3 grateful to UTN-FRC and CONICET for the financial support. JPP acknowledges  
4 MICIN for financial support through project PID2019-107968RB-I00.  
5 To the SEGIB-Carolina Foundation for Scholarship Research Stays program.  
6 Madrid - Spain. 2020.

7

## 8 References

- 9 [1] J. Beck, J. Vartuli, W. Roth, M. Leonowicz, C. Kresge, K. Schmidt, C. Chu, D.  
10 Olson, E. Sheppard, S. McCullen, J. Higgins, J. Schenkler, *J. Am. Chem. Soc.* 114  
11 (1992) 10834.
- 12 [2] E. Vaschetto, G. Pecchi, S. Casuscelli, G. Eimer. *Microp. and Mesop. Mater.*  
13 200 (2014) 110.
- 14 [3] V. Elías, M. Oliva, E. Vaschetto, S. Urreta, G. Eimer, S. Silveti. *J. of Magnetism*  
15 *and Magnetic Materials* 322 (2010) 3438.
- 16 [4] V. Elías, M. Crivello, E. Herrero, S. Casuscelli, G. Eimer, *J. Non. Cryst. Solids*  
17 355 (2009) 1269.
- 18 [5] V. Elías, G. Ferrero, R. Oliveira, G. Eimer, *Microporous Mesoporous Mater.* 236  
19 (2016) 218.
- 20 [6] S. Aspromonte, A. Tavella, M. Mariño, M. Albarracín, C. Osella, A. Boix, *XX*  
21 *CAC* (2017), trabajo N°: 234.
- 22 [7] A. Akinjokun, T. Ojumu, A. Ogunfowokan <http://dx.doi.org/10.5772/63463>  
23 (2016) 103. <https://www.intechopen.com/chapters/50761>
- 24 [8] C. P. Canlas, T.J. Pinnavaia. *RSC Advances*. 2012;2(19):7449–55.
- 25 [9] B. Thomas, N. Baccile, S. Masse, C. Rondel, I. Alric, R. Valentin. *Journal of*  
26 *Sol-gel Science and Technology*. 2011;58(1):170-4.
- 27 [10] C. Rondel, I. Alric, Z. Mouloungui, J-F Blanco, F. Silvestre. *Journal of*  
28 *Surfactants and Detergents*. 2009;12(3):269–75.
- 29 [11] X. Wei Dong, Y. Yu Xiang, C. Jing, W. Zhaolun, L. Xiang Nong. *Journal of the*  
30 *American Ceramic Society*. 2008;91(5):1517-21.

- 1 [12] A. El Kadib, M. Bousmina. *Chemistry-A European Journal*. 2012;18(27):8264-  
2 77.
- 3 [13] V. Pedroni, P. Schulz, M. G. de Ferreira, M. Morini. *Colloid and Polymer*  
4 *Science*. 2000;278(10):964-71.
- 5 [14] T. Witoon, M. Chareonpanich, J. Limtrakul. *Materials Letters*.  
6 2008;62(10):1476–9.
- 7 [15] D-W Lee, M-H Jin, JC Park, C-B Lee, D Oh, S-W Lee. *Scientific reports*.  
8 2015;1–5.
- 9 [16] J. Peña, E. Cardona, L. Rios, *Dyna* 75 (2008) 207.
- 10 [17] A. Dubois, L. Blacoutureilan Bilan de présence des micropolluants dans les  
11 milieu aquatiques continentaux. Période 2007–2009, Commissariat general au  
12 developpement durable. N° 54, 2011.
- 13 [18] B. Barja, J. Herszage, A.M. dos Santos, *Polyhedron* 20 (1821) (2001).
- 14 [19] D. Robert, S. Malato, *Solar photocatalysis: a clean process for water*  
15 *detoxification*, *Sci. Total Environ.* 291 (2002) 85–97.
- 16 [20] K. Kyoung-Hun, I. Son. -Ki, *J. Hazard. Mater.* 186 (2011) 16–34.
- 17 [21] E. Vaschetto, M. Sicardi, V. Elías, G. Ferrero, P. Carraro, S. Casuscelli, G.  
18 Eimer, *Adsorption* 25 (2019) 1–8.
- 19 [22] E. Vaschetto, P. Ochoa Rodríguez, S. Casuscelli, V. Elías, G. Eimer. *Catalysis*  
20 *Today* 394-396 (2022) 143–149.
- 21 [23] L. Bing Sun, J. Hui Kou, Y. Wang, J. Hua Zhu, Z. Gang Zou *Inorg. Chem.* 47  
22 (2008) 4199.
- 23 [24] V. Elías, P. Ochoa Rodriguez, E. Vaschetto, G. Pecchi, C. Huck-Iriart, S.  
24 Casuscelli, G. Eimer. *Molecular Catalysis*. 481 (2020) 1.
- 25 [25] M. Rabiej, A. Palevicius, A. Dashti, S. Nasiri, A. Monshi, A. Vilkauskas and G.  
26 Janusas. *Materials*. 13 (2020) 4380.
- 27 [26] X. Jiang, N. Liu, R. Assink, Y. Jiang and C. Brinker. *J. of Nanomaterials*. 2011  
28 (2011) 1.
- 29 [27] C. Cheng, Z. Luan, J. Klinowski, *Langmuir* 11 (1995) 2815.
- 30 [28] N. Cuello, V. Elías, M. Crivello, C. Torres, M. Oliva, G. Eimer. *Microporous and*  
31 *Mesoporous Mater.* 203 (2015). 106.

- 1 [29] V. Elías, E. Vaschetto, K. Sapag, M. Oliva, S. Casuscelli, G. Eimer. *Catal*  
2 *Today* (2011) 172-1:58–65
- 3 [30] Y. Lu, J. Zheng, J. Liu, J. Mu. *Microporous Mesoporous Mater* 106: (2007) 28–  
4 34
- 5 [31] Y. Wang, Q. Zhang, T. Shishido, K. Takehira (2002). *J Catal* 209:186–196
- 6 [32] S. Bordiga, S. Coluccia, C. Lamberti, L. Marchese, A. Zecchina, F. Boscherini,  
7 F. Bufo, F. Genoni, G. Leofanti, G. Petrini, G. Vlaic, *J. Phys. Chem.* 98 (1994)  
8 4125–4132.
- 9 [33] G. Ricchiardi, A. Damin, S. Bordiga, C. Lamberti, G. Spano, F. Rivetti, A.  
10 Zecchina, *J. Am. Chem. Soc.* 121 (2001) 11409–11419.
- 11 [34] A. De Stefanis, S. Kaciulis, L. Pandolfi, *Microporous Mesoporous Mater.* 99  
12 (2007) 140–148.
- 13 [35] L. Shiquan, Q. Wang, P. Van Der Voort, P. Cool, *J. Magn. Magn. Mater.* 280  
14 (2004) 31–36.
- 15 [36] S. Bordiga, R. Buzzoni, F. Geobaldo, Lamberti E. Giamello, A. Zecchina, G.  
16 Leofanti, G. Petrini, G. Tozzola, and G. Vlaic. *Journal of catalysis* 158, (1996) 486–  
17 501.
- 18 [37] L. Chmielarz, P. Kustrowski, R. Dziembaj, P. Cool, E. Vansant, *Appl. Catal.* 62  
19 (2006) 369–380.
- 20 [38] D. Beydoun, R. Amal, G. Low, S. MacEvoy, *J. Nanopart. Res.* 1 (1999) 439–  
21 458.
- 22 [39] S. Liu, Q. Wang, P. Van Der Voort, P. Cool, E. Vansant, M. Jiang. *J Magn*  
23 *Magn Mater* 280 (2004)31–36
- 24 [40] V. Elías, T. Benzaquén, P. Ochoa Rodríguez, N. Cuello, A. Tolley, G. Eimer.  
25 *Catalysis Letters* (2020) 150:196–208.
- 26 [41] M. Caetano, T. Ramalho, D. Botrel, E. da Cunha, W. Carvalho de Mello. *Int. J.*  
27 *Quantum Chem.* 112 (2012) 2752–2762.
- 28 [42] C. Coutinho, L. Henrique Mazo, *Quim. Nova* 28 (2005) 1038–1045.
- 29 [43] W. Harris, R. Douglas Sammons, R. Grabiak, A. Mehrsheikh, M. Bleeke. *J.*  
30 *Agric. Food Chem.* 60 (2012) 6077–6087.
- 31 [44] V. Subramaniam, P. Hoggard, *J. Agric. Food Chem.* 36 (1988) 1326–1329.

- 1 [45] H. Li. University of Delaware, United States, 2018.
- 2 [46] J. Sheals, S. Sjoberg, P. Persson. 36 (2002) 3090–3095.
- 3 [47] C.V. Waiman, M.J. Avena, A.E. Regazzoni, G.P. Zanini. J. Colloid Interface
- 4 Sci. 394 (2013) 485–489.
- 5 [48] R.A. Sheldon, J.K.Kochi Metal-Catalyzed, Oxidations of organic compounds.
- 6 Mechanistic Principles and Synthetic Methodology Including Biochemical
- 7 Processes, Academic Press, London, 1981.
- 8 [49] R.A. Sheldon, J.K.Kochi Metal-Catalyzed, Oxidations of Organic Compounds
- 9 in the Liquid Phase: a Mechanistic Approach, Academic Press,, London, 1981.
- 10 [50] E.G. Vaschetto, J.D. Fernandez, S.G. Casuscelli, G.A. Eimer, Catal. Lett.
- 11 143(2013) 333.
- 12

## Highlights

- Mesoporous silica structures from biomass-derived renewable molding were synthesized
- The mesoporous structure achieved was corroborated by XRD and physisorption of N<sub>2</sub>.
- The solids were prepared by wet impregnation with and direct incorporation with Fe
- Herbicide degradation / fragmentation levels of around 70% were achieved
- The reaction was carried by catalytic wet air oxidation at atmospheric P and room T

**Declaration of interests**

The authors declare that they have no known competing financial interests or personal relationships that could have appeared to influence the work reported in this paper.

The authors declare the following financial interests/personal relationships which may be considered as potential competing interests:

Journal Pre-proof